Development of cooperativity in the local segmental dynamics of poly(vinylacetate): synergy of thermodynamics and intermolecular coupling[☆]

K.L. Ngai*, C.M. Roland

Naval Research Laboratory, Washington, DC 20375-5320, USA

Abstract

The properties of the α- and Johari–Goldstein β-relaxations in conjunction with configurational entropy data are used to show how cooperativity of the dynamics of poly(vinylacetate) develops as temperature is decreased towards T_g from above. Such behavior is also characteristic of small molecule glass-forming liquids, demonstrating that the combined effects of configurational entropy changes and intermolecular coupling underlie structural relaxation phenomena. Any theoretical model must include both thermodynamics and many-body dynamics in order to accurately describe the general properties of the glass transition. © 2001 Elsevier Science Ltd. All rights reserved.

Keywords: Poly(vinylacetate); Local segmental dynamics; Intermolecular coupling

1. Introduction

There have been various attempts, most prominently the free volume theories [1,2] and the configurational entropy model of Adam and Gibbs (AG) [3,4], to explain the temperature dependence of the molecular dynamics of glass-forming supercooled liquids *solely* in terms of changes in some thermodynamic quantity. Free volume theory identifies this thermodynamic quantity to be the difference between the total volume, v, and the occupied volume, v_o, which decreases with decreasing temperature. According to the Doolittle free volume equation, the structural relaxation time, τ_α, is then,

$$\tau_\alpha(T) = A \exp\left[\frac{B}{(v - v_o)/v_o} \right] \quad (1)$$

Assuming v_o to be insensitive to temperature and that $v = v_o + \alpha_p(T - T_\infty)$, where α_p is the volume expansion coefficient and T_∞ the temperature at which the free volume would go to zero (if not for intervention of the glass transition), Eq. (1) yields the Vogel–Fulcher–Tammann–Hesse

(VFTH) equation,

$$\tau_\alpha(T) = A \exp\left[\frac{(Bv_o/\alpha_p)}{T - T_\infty} \right] \quad (2)$$

and the equivalent Williams–Landel–Ferry equation [2] for the shift factor, a_T, defined as the ratio $\tau_\alpha(T)/\tau_\alpha(T_o)$, where T_o is an arbitrary reference temperature.

An alternative approach is the theory of AG [3,4], in which the relevant thermodynamic quantity a configurational entropy, S_c, defined as the difference in configurational entropy between the supercooled liquid and the crystal, S_c. The structural relaxation time is given by

$$\tau_\alpha(T) = \tau_\infty \exp(C/TS_c) \quad (3)$$

where τ_∞ is the relaxation time at infinite temperature and C a constant.

The principal results of the two theories, Eqs. (2) and (3), respectively, account for the non-Arrhenius temperature dependence of the relaxation time and transport coefficients. Eq. (3) can be cast into the form of Eq. (2) if the assumption is made that the specific heat of glass-forming liquids is approximately independent of temperature. However, as recently discussed by Johari [5], neither the specific heat of the liquid nor the difference in specific heats of the equilibrium melt and the glass is temperature invariant near the vitrification temperature, T_g. Hence, the crucial approximation made by AG [3,4] to connect the temperature variation of S_c with the VFTH temperature dependence of the viscosity or τ lacks experimental justification.

These two theories are confined to the temperature dependence of the relaxation time or transport coefficients, and do not address most other dynamic properties [6]. Moreover, even for the temperature dependence of the relaxation time, Eq. (2) or (3) do not accurately describe experimental data for glass-formers obtained over a broad temperature range [2,6–15]. Improvements to these theories have been proposed, such as that of Cohen and Grest [16], but usually involve additional parameters and assumptions. It is remarkable that 30-year old theories are considered by many to be viable descriptions of the dynamics of supercooled liquids, capturing the essential physics. An example is the recent work by Ito et al. [17], suggesting that the configurational entropy alone can predict trends in the temperature dependence of $\tau_\alpha(T)$ among glass-formers. This proposal has been refuted by experimental data for both small molecules [18] and polymers [19].

We have pointed out that a viable explanation of not only the temperature dependence of the relaxation time, but other salient dynamic properties of glass-formers as well, cannot be based on thermodynamics alone [15,20]. The effects of intermolecular coupling due to interaction between molecules must be considered. A theory that explicitly includes intermolecular coupling is the coupling model (CM) [21–29]. A recent version of the CM, based on non-linear Hamiltonian dynamics (chaos), brought out the effects of intermolecular coupling by reproducing dynamic properties similar to supercooled liquids [24]. Appreciation of the importance of intermolecular coupling can be gleaned from examination of experimental quantities indicative of coupled dynamics:

(i) The degree of departure from exponential decay characterized by the coupling parameter, n, appearing in the exponent of the Kohlrausch–William–Watts function [30,31],

$$\phi(t) = \exp[-(t/\tau_\alpha)^{1-n}], \quad 0 \leq n < 1, \tag{4}$$

which often gives a good description of the time dependence of the measured correlation function. In the CM [21–29], n increases with increasing molecular interaction strength [32] and comparisons of the values of n for different glass-formers at their respective T_g, reveals differences in intermolecular coupling strength. The temperature dependence of n also reflects how intermolecular coupling changes with temperature.

(ii) The departure of temperature dependence of τ or the viscosity η from that given by the VFTH equation, Eq. (2). In fact, data taken over a wide range of temperature above T_g usually show an Arrhenius temperature dependence at high temperatures $T > T_A$, a VFTH dependence in the intermediate range $T_A > T > T_B$, and another VFTH dependence in the range $T_B > T > T_g$ [8–16,20]. The apparent activation enthalpy, $H \equiv R[\mathrm{d}(\log_e \tau_\alpha)/\mathrm{d}(1/T)]$, has a physically meaningful, constant value in the Arrhenius regime ($T > T_A$), then increasing as temperature is lowered below T_A, moderately in the intermediate temperature regime ($T_A > T > T_B$) and significantly in the final regime ($T_B > T > T_g$). A quantity closely related to H is the dimensionless steepness index [15,20],

$$m = \mathrm{d}(\log_{10} \tau_\alpha)/\mathrm{d}(T_g/T) \tag{5}$$

which exhibits the same behavior as H over the three temperature regimes. Comparison of the temperature dependence of different glass-formers can be made through their respective values of m, either at $T_g/T = 1$ [33] or more completely by the dependence on T_g/T.

(iii) The temperature dependence of n also shows signs of crossovers in the three regimes. For $T > T_A$, n is nearly equal to or exactly zero. There is only a slight increase in n as temperature is decreased from T_A down to T_B, typically up to a value around 0.2. A substantial and rapid increase of n occurs as temperature falls below T_B [14].

(iv) It has been found recently that the Johari–Goldstein (JG) secondary or β-relaxation [34] found in most glass-formers, including polymers without side groups, bears an interesting relation to the structural or α-relaxation [35–37]. The JG process observed below T_g usually has an Arrhenius temperature dependence. If this Arrhenius dependence is used to extrapolate the most probable JG relaxation time, τ_β, to temperatures above T_g, for many glass-formers τ_β becomes equal to τ_α at a temperature, T_β, which turns out to be very close to T_B. Another interesting relation is that at T_g, the values of τ_β and n are strongly correlated. These cross correlations between the JG β-relaxation and the α-relaxation can be interpreted in the context of the CM. The JG β-*process* is unaffected by cooperativity of the molecular motions, and in this fashion is similar, though not identical to, the primitive relaxation in the CM. This correlation provides an estimate of τ_β at temperatures above T_g, using the equation of the CM,

$$\tau_\alpha = [t_c^{-n} \tau_0]^{1/(1-n)} \tag{6}$$

in which the crossover time, t_c, is about 2 ps for molecular liquids [26,35,36]. The primitive (uncoupled) relaxation time τ_o, and hence approximately τ_β, can be calculated from experimental determined values for τ_α and n.

(v) The molar configurational entropy, $S_c(T)$, of glass-formers can be obtained from calorimetric data [38,39]. On decreasing temperature, the ratio, $S_{c\infty}/S_c(T)$ increases monotonically from unity at high temperatures ($S_{c\infty}$ is the value of $S_c(T)$ in the limit of very high temperatures). In the Adam–Gibbs theory, this ratio gives the number of molecules in the cooperative rearranging region, z^* of their model. Although the Adam–Gibbs theory by itself cannot explain dynamic properties [5,6,7–16], it is still useful to examine how the thermodynamic quantity z^* changes with temperature, as well as its variation among glass-formers. Remarkably, $z^*(T)$ exhibits crossover properties similar to $n(T)$ and $m(T)$ at both T_A and T_B. Specifically, $z^*(T)$ is close to unity for $T > T_A$. On decreasing temperature, z^* increases

monotonically, up to a value of about two in the region $T_A > T > T_B$. This is followed by a more significant rise in the region $T_B > T > T_g$. The similar temperature dependences of $z^*(T)$, $n(T)$ and $m(T)$ reveal a synergy between thermodynamics and intermolecular coupling in governing the dynamic properties of glass-formers.

The phenomenology of the intermolecularly coupled dynamics of glass-formers, summarized in (i)–(v) above, have been established from data on small molecule super-cooled liquids and melts. Collectively, they have not been demonstrated for a polymer. The objective of this work is to show that most of the characteristics (i)–(v) are exhibited by the amorphous polymer poly(vinylacetate).

2. Relaxation map: α-relaxation

Polyvinylacetate (PVAc) is among the polymeric materials first studied by dielectric and mechanical spectro-scopic techniques [40]. The earlier data cover only a limited frequency range, so that they cannot be used to test the characteristics (i)–(v). Also, the structural relaxation of PVAc is sensitive to water content, so that dry samples have to be used for reliable data acquisition. For the present purpose, we take the recent isothermal dielectric relaxation measurements of dried PVAc ($M_w \approx 15\,000$ g/mol; $M_w/M_n \approx 3$; $T_g \approx 300$ K) by Stickel [10], which encompass a large frequency range from $2 \times 10^{10} > f > 10^{-2}$ Hz. The α-relaxation frequencies, f, defined by the maximum of the dielectric loss function, $\epsilon''(f)$, are plotted against temperature in Fig. 1 (filled circles). From the data we calculate the quantity $[\mathrm{d}\log(f/\mathrm{Hz})/\mathrm{d}T]^{-1/2}$, which is also plotted in Fig. 1. As pointed out by Stickel [8–10], if the α-relaxation frequency has the VFTH temperature depen-dence,

$$\log f = A - \frac{B}{T - T_\infty}, \tag{7}$$

then

$$\left(\frac{\mathrm{d}\log f}{\mathrm{d}T}\right)^{-1/2} = B^{-1/2}(T - T_\infty) \tag{8}$$

yields a straight line when plotted against T. This allows B and T to be deduced from the slope and intercept. However, as seen in Fig. 1, $[\mathrm{d}\log(f/\mathrm{Hz})/\mathrm{d}T]^{-1/2}$ versus T for PVAc is not linear. Data well below 383 K lie on one straight line, and data well above 383 K lie on another. This means that two VFTH equations are required to describe the full temperature dependence of the α-relaxation, with the temperature dependence changing in the vicinity of $T_B = 383$ K. The α-relaxation frequencies calculated from the two VFTH equations are shown by the dotted and solid curves in Fig. 1. These results, noted by Stickel [10], show that PVAc possesses the characteristic (ii). At present, there is no α-relaxation data for PVAc at frequencies higher than 10^8 Hz, so the crossover at T_A. Fig. 2 shows the varia-
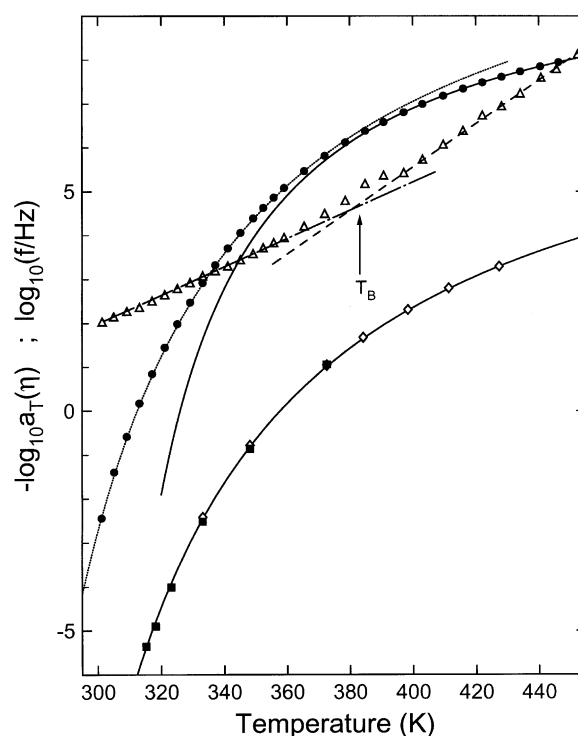

Fig. 1. Semilogarithmic plot of the frequency of the maximum in the dielectric loss versus temperature. Filled circles are data given by Stickel [10], and the curves represent the two VFTH equations, as described in the text. The open triangles are the values of $[d\log(f/\mathrm{Hz})/\mathrm{d}T]^{-1/2}$ obtained from the data. The two dashed lines needed to fit these data intersect at the crossover temperature $T_B = 383$ K. The open diamonds and the filled squares are the shift factors, $\log a_T$, for the viscosity and the terminal dispersion, respectively from Ref. [42], after changing their sign and shift-ing by seven decades.

tion of the steepness index, m, calculated from the dielectric data using Eq. (5).

Recently, Schönhals [41] demonstrated for several small molecule glass-formers that a plot of the dielectric relaxa-tion strength of the α-relaxation, $\Delta\epsilon$, against $\log_{10}(f)$ also reveals the crossover at T_B. Fig. 3 shows such a plot for PVAc, using the data of Stickel [10]. It is apparent that $\Delta\varepsilon$ decreases as a function of $\log_{10}(f)$ much more rapidly in the regime $T > T_B$ than for $T < T_B$, consistent with the crossover at T_B seen in Fig. 1.

Since the PVAc is an entangled polymer, it exhibits a terminal dispersion and viscosity that are determined by chain motions having length scales of the order of the radius of gyration. Such a large length scale is quite different from the monomer size distance associated with the local segmental or α-relaxation. Plazek [42] measured the term-inal dispersion for PVAc over a broad temperature range, and found that its temperature dependence is indistinguish-able from that of the viscosity. The time–temperature shift factors reported by Plazek [42] are plotted in Fig. 1, after a change in sign and upward shift by seven decades to allow comparison to the dielectric data. Good agreement between the temperature dependences of the terminal dispersion
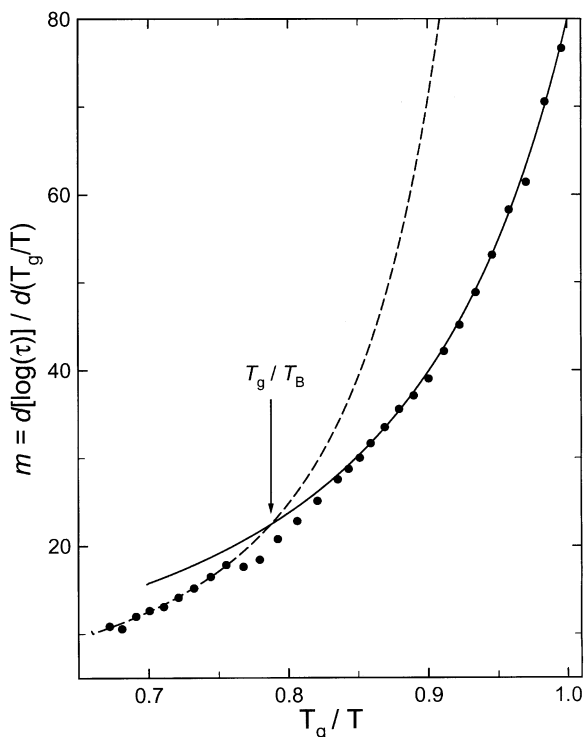
Fig. 2. The steepness index, $m = [\mathrm{d}\log \tau/\mathrm{d}(T_g/T)]$, calculated from experimental τ as a function of T_g/T. Here T_g is taken to be 300 K, the temperature at which $\tau = 100$ s. The intersection of the curves at $T_B = 383$ K is obtained by taking the derivative the two VFTH fits to relaxation times shown in Fig. 1.
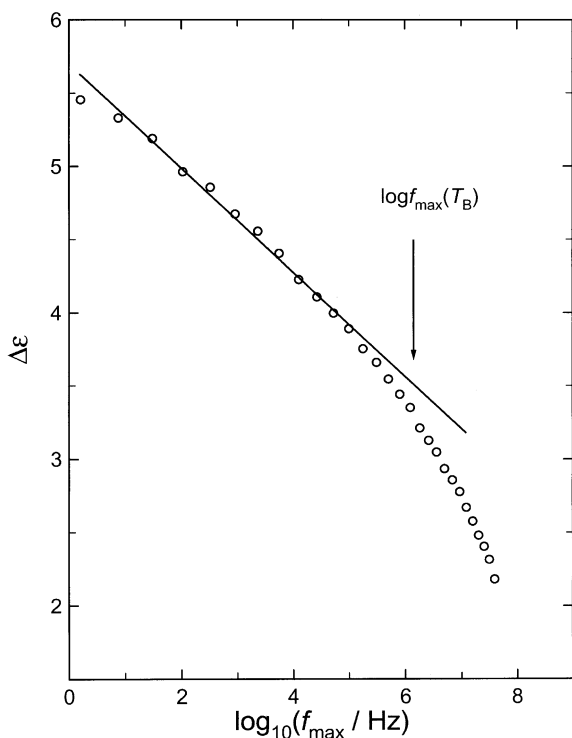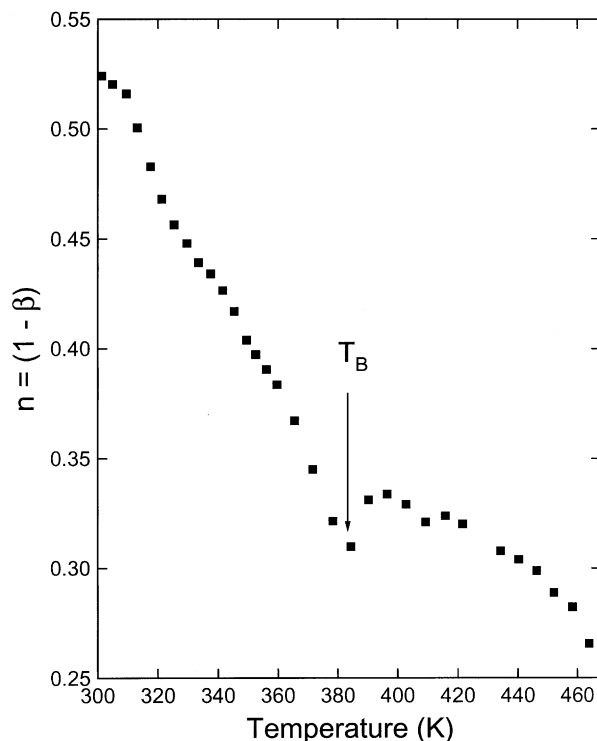

Fig. 4. The temperature dependence of $n(T)$ for PVAc obtained from Eq. (9).

(filled squares) and the viscosity (open diamonds) is observed, so that we treat these collectively, as shift factors $\log a_T$. In contrast to the dielectric α-relaxation frequencies, Plazek found that a single VFTH function, $\log a_T = -15.47 + 928/(T + 25)$ where T is given in °C, fit his experimental data. This is demonstrated in Fig. 1 by the solid curve through all data points, which span a range of 8.6 decades in $\log a_T$. There is no crossover of $\log a_T$ to another VFTH form at T_B. This interesting difference between the temperature dependence of the α-relaxation and the terminal dispersion and viscosity is revisited in Section 6.

3. Temperature dependence of *n*

Stickel [10] reported the full-width at half-maximum of the dielectric loss peak of PVAc normalized to that of an ideal Debye loss peak, w, as a function of temperature. The dielectric dispersion of the α-relaxation of PVAc is then be fit to the Fourier transform of the time derivative of the KWW correlation functions, Eq. (4) [43]. An approximate relation between w and n was given by Dixon [44]

$$n = 1.047(1 - w^{-1}) \tag{9}$$

The $n(T)$ calculated according to Eq. (9) are shown in Fig. 4. T_B, at which τ_α transitions from one VFTH to another, is indicated. Similar to small molecular glass-formers, Fig. 4 reveals that for temperatures above T_B, n is small and

Fig. 3. Semi-logarithmic plot of the dielectric relaxation strength of the α-relaxation of PVAc versus the frequency of the maximum in the dielectric loss. The marked decrease of $\Delta\varepsilon$ reveals the crossover at T_B.
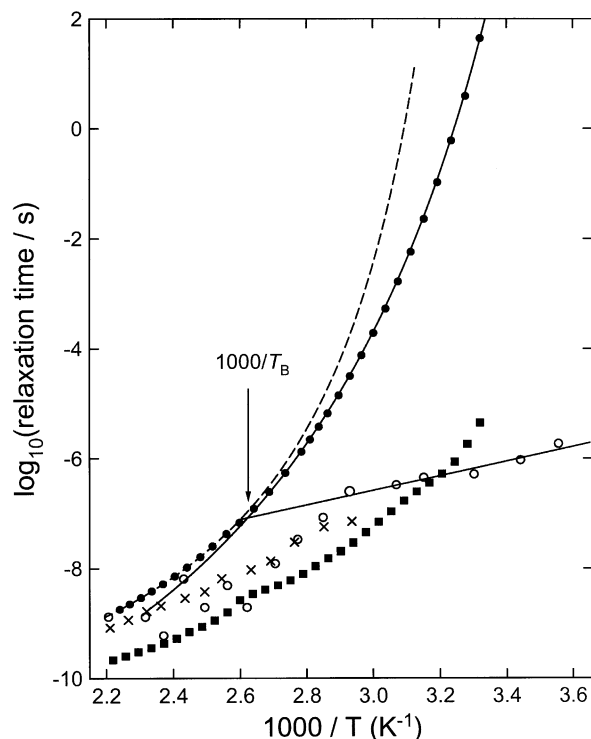
Fig. 5. Logarithm of the dielectric relaxation times, $\log_{10}(\tau_\alpha/s)$ of PVAc plotted versus reciprocal. Filled circles are data of Stickel [10], and the curves through some of the data are the relaxation times corresponding to the two VFTH equations in Fig. 1. Open circles are τ_βs obtained by assuming the β-relaxation and the α-relaxation make additive contributions to the dielectric spectra [50], while the crosses are τ_βs obtained by assuming the dielectric spectra is a convolution of the α- and β-relaxations [50]. The straight line drawn through the open circles at lower temperature intersects $\log_{10}(\tau_\alpha/s)$ at a value close to T_B. The filled squares are the primitive relaxation times, τ_0 calculated by Eq. (6) from the τ_α using the values of n from Fig. 4 with $t_c = 2$ ps.

decreases slowly with increasing temperature, while for temperatures below T_B, n increases rapidly, attaining a significantly larger value at T_g. Thus, PVAc exhibits the characteristics (i) and (iii) of small molecule glass-formers.

Unlike small molecular liquids, however, the primitive α-relaxation of a polymer does not decay exponentially (i.e. Debye relaxation) with time because of the intramolecular cooperativity arising from bonded interactions along the chain [45–48]. It has been shown [47] that at higher temperatures for which τ_α becomes small, this intramolecular cooperativity contributes to the departure from exponential relaxation of the α-relaxation as measured by w. This additional contribution may be the origin of the slightly larger value of n for PVAc in comparison with small molecular glass-formers (i.e. at temperatures above T_B, n is as high as 0.32 for PVAc, whereas $n(T) < 0.2$ for small molecular glass-formers) [14,20]. This idea is supported by the comparable width of the dielectric loss peaks for PVAc in dilute solution [49], which certainly reflects the local chain motion. In other words, the actual intermolecular coupling parameter at temperatures higher than T_B is smaller than the values of n calculated from Eq. (9) and reported in Fig. 4.

Nevertheless, with falling temperature, the crossover at T_B from a slowly varying and small value of n to a rapid increase of n towards a large value at T_g supports the interpretation of substantial intermolecular cooperativity arising below T_B in PVAc.

4. Relaxation map: β-relaxation and the primitive α-relaxation

Of primary interest is whether the relationship between the relaxation times for the β-process and the CM's primitive relaxation, observed for small molecular glass-formers (iv) above, pertains to PVAc. For this purpose, we use recently published β-relaxation data [50] for temperatures both below and above T_g (Fig. 5). Earlier data for the β-relaxation of PVAc [10,40], obtained at temperatures further below T_g, are not as useful for this purpose. The open circles in Fig. 5 are τ_βs obtained by assuming the β-relaxation and the α-relaxation make additive contributions to the dielectric spectra [50,51]. The crosses are τ_βs obtained by assuming the dielectric spectrum is a convolution of the β- and α-relaxations [52]. The difference between the two methods is less than the scatter in the data. The lower temperature data exhibit an apparent Arrhenius dependence, as indicated by the straight line, which intersects τ_α at a temperature T_β close to T_B.

The primitive relaxation time, τ_0, can be calculated by Eq. (6), using experimental values for n and τ_α, with $t_c = 2$ ps [25,26]. The results (filled squares) are shown in Fig. 5. τ_0 and τ_β are within an order of magnitude of one another. Smaller values of n than those taken directly from Fig. 4 would yield better agreement. In the previous section, we suggested why n may be overestimated in the temperature region in which τ_α is small (see also Fig. 3 in Ref. [46]). In any event, we can conclude that PVAc exhibits the characteristic properties embodied in (iv) for small molecular glass-formers.

5. Thermodynamic property

The configurational entropy is calculated as

$$S_c(T) = \int_0^T \frac{\Delta C_p}{T}\,dT, \tag{10}$$

where ΔC_p is the difference in heat capacity between the liquid and crystalline states. Experimental heat capacities for amorphous PVAc have been measured from 80 to 300 K [37]. The polymer degrades at elevated temperatures [53], but values can be obtained by linear extrapolation [37]. It is common to use the entropy of fusion as a reference point; that is, S_c is defined as the change of the fusion entropy with temperature. However, since the entropy of fusion is unknown for amorphous PVAc, the absolute entropy is likewise unknown. Using reported thermodynamic data for PVAc [38], S_c is calculated and shown in
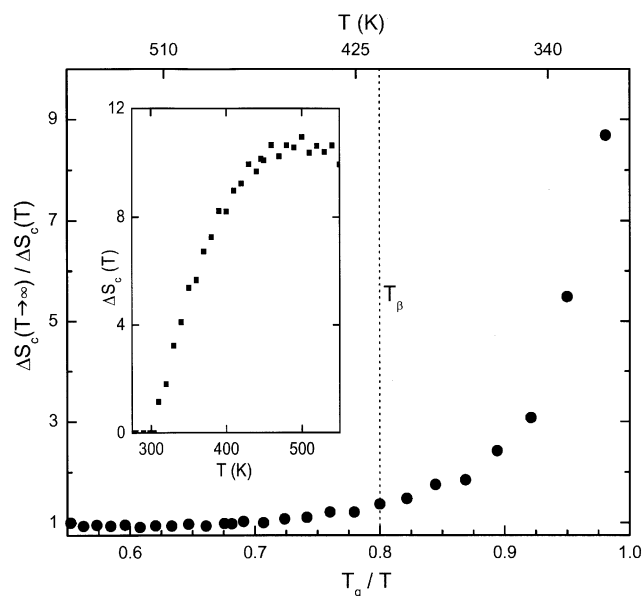
Fig. 6. The inverse configurational entropy normalized by the limiting value at high temperature for PVAc. The vertical dashed line indicates the merging temperature. The unnormalized configurational entropy is shown in the inset.

the inset to Fig. 6. At high temperature a limiting value, $S_c(T \to \infty) = 9.9$, is attained. According to the model of AG [4], the ratio of this quantity to $S_c(T)$ represents the average number of chain units in the cooperatively rearranging region (CRR), z^*. We plot this ratio $S_c(T \to \infty)/S_c$ in Fig. 6 versus the temperature variable T_g/T, where now $T_g = 304$ K from Ref. [39] is used.

It is clear by inspection of Fig. 6 that $S_c(T \to \infty)/S_c$ is nearly unity at high temperatures, increasing only slightly with decreasing temperature to a value of about 1.5 at T_B. Below T_B, the increase of z^* is substantial, becoming more rapid with decreasing temperature. This change of temperature dependence of $S_c(T \to \infty)/S_c$ across T_B corresponds to the characteristic (v) of small molecular glass-formers.

Although the available capacity data for PVAc is sparse, especially at higher temperatures, it is tempting to interpret the behavior in Fig. 5 in light of the AG model. Near T_g, $S_c(T \to \infty)/S_c$ attains a value on the order of nine. This exceeds the values reported, for example, for *ortho*-terphenyl and toluene [18,20,38]. The size of the CRR, or length scale of the spatial heterogeneity, at T_g is expected to fall in the range 2–6 nm [54–56]. This corresponds to a distance along the backbone in PVAc equal to 6–20 repeat units (C–C bond distance equals 0.154 nm). While this is consistent with the value of $S_{c,\infty}/S_c$ near T_g, nine chain units of PVAc seems unrealistically large for such local motion.

6. Discussion

Most of the general dynamic properties of small molecu-

lar glass-formers (i)–(v) can be observed in the amorphous polymer, PVAc. These properties provide strong evidence for a synergy between thermodynamics (configurational entropy or free volume) and intermolecular coupling in the development of cooperativity and consequent slowing down of the molecular motions. Both aspects are required for an adequate description of the diverse properties. Neither the Adam–Gibbs model nor free volume theory is adequate, because the invoked mechanisms involve only thermodynamic quantities.

At high temperatures ($T > T_A$), neither thermodynamics nor intermolecular coupling has any effect. The molecules execute independent (uncoupled) motion, which is thermally activated with an Arrhenius dependence. For PVAc, data is lacking at sufficiently high temperatures for this regime to be observed. However, the configurational entropy at high temperatures indicates that $z^* \to 1$, i.e. independent molecular motion, for $T > 450$ K. Thus, 450 K serves as a crude estimate of T_A. In the intermediate temperature range, $T_A > T > T_B = 383$ K, all quantities, including n, m, and $S_c(T \to \infty)/S_c$, increase weakly with decreasing temperature. As temperature is reduced below T_B, these quantities show a more significant and rapid increase until T_g is reached.

The variation of z^* with temperature comes entirely from thermodynamics data. Thermodynamics, arising from the entropy crisis, is a fundamental driving force. The similarity of the temperature dependences for $z^*(T)$ and $n(T)$ and $m(T)$ suggests that thermodynamics, coupled with the effect it has on the dynamics via intermolecular cooperativity, gives rise to the generally observed temperature dependence of $[1 - n(T)]$. We have previously [15] modified the Adam–Gibbs theory to incorporate intermolecular coupling. Using AG to describe the temperature dependence of the CM's primitive relaxation time, τ_o, the effect of intermolecular coupling is then accounted for by Eq. (6). It is evident from the results for PVAc presented herein that the local segmental α-relaxation of polymers may likewise be described by the modified Adam–Gibbs theory.

As shown in Fig. 1, the temperature dependences of the local segmental α-relaxation frequency, $\log(\tau_\alpha)$, and the shift actor, $\log(a_T)$, for the terminal relaxation or viscosity are different in high molecular weight PVAc. The former requires two VFTH equations to describe the regimes $T > T_B$ and $T_B > T$, while the latter exhibits no crossover at T_B, so that a single VFTH equation suffices. This difference can be accounted for in terms of the different coupling parameters, n for the α-relaxation and n_η for the terminal relaxation [29]. We have seen that n is temperature dependent (Fig. 4) with a marked change at T_B. On the other hand, n_η is temperature independent and for entangled polymers has a value of about 0.41 [57,58]. The temperature independence of n_η is a manifestation of thermo-rheological simplicity of the terminal dispersion of linear entangled polymers [3,42]. It can also be deduced from the fact that an entanglement coupling involves a larger length-scale, corresponding

to the molecular weight between entanglements, than does z^*. This implies that the entanglement interactions are insensitive to changes in the size of the CRR with temperature. In the CM, the primitive shift factors of the two relaxation processes have the same temperature dependence [29], but their observed temperature dependences, as determined by Eq. (5), differ. Thus, the differing temperature dependences of $\log(\tau_\alpha)$, and $\log(a_T)$ are a consequence of the temperature variation of n for the α-relaxation and the lack of same for n_η.

7. Conclusions

Various phenomena involving the local segmental relaxation, the Johari–Goldstein β-relaxation and the (hypothetical) primitive relaxation of the CM, previously known to be characteristics of small molecular glass-forming liquids, are observed herein for poly(vinylacetate), an amorphous polymer. The generality of these properties indicates that synergy of thermodynamics and intermolecular coupling (many-body effects) underlies the dynamic properties of supercooled liquids and melts. Accordingly, theories of structural relaxation must take into consideration both thermodynamics and intermolecular coupling in order to successfully account for these properties. The Adam–Gibbs theory modified to incorporate the coupling model is an example of such a theory.

Acknowledgements

References

[1] Doolittle AK. J Appl Phys 1951;22:1471.
[2] Ferry JD. Viscoelastic properties of polymers. 3rd ed. New York: Wiley, 1980.
[3] Adam G, Gibbs JH. J Chem Phys 1965;43:139.
[4] DiMarzio EA, Yang AJM. J Natl Inst Standards Technol 1997;102:135.
[5] Johari GP. J Chem Phys 2001 (in press).
[6] Ngai KL. J Non-Cryst Solids 2000;275:7.
[7] Ngai KL, Magill JH, Plazek DJ. J Chem Phys 2000;112:1887.
[8] Stickel F, Fischer EW, Richert R. J Chem Phys 1995;102:6251.
[9] Stickel F, Fischer EW, Richert R. J Chem Phys 1996;104:2043.
[10] Stickel F. PhD thesis, Johannes Gutenberg University, Mainz, Germany (Shaker, Aachen, 1995).
[11] Hansen C, Stickel F, Berger T, Richert R, Fischer EW. J Chem Phys 1977;107:1086.
[12] Hansen C, Stickel F, Richert R, Fischer EW. J Chem Phys 1998;108:6408.
[13] Richert R, Angell CA. J Chem Phys 1998;108:9016.
[14] León C, Ngai KL. J Phys Chem 1999;103:4045.
[15] Ngai KL. J Phys Chem 1999;103:10 684.
[16] Cohen MH, Grest G. Phys Rev B 1979;20:1077.
[17] Ito K, Moynihan CT, Angell CA. Nature 1999;398:492.
[18] Ngai KL, Yamamuro O. J Chem Phys 1999;111:10 403.
[19] Roland CM, Santangelo PG, Ngai KL. J Chem Phys 1999;111:5593.
[20] Ngai KL. J Chem Phys 1999;111:3639.
[21] Ngai KL. Comments Solid State Phys 1979;9:127.
[22] Tsang KY, Ngai KL. Phys Rev E 1997;54:3067.
[23] Tsang KY, Ngai KL. Phys Rev E 1997;56:R17.
[24] Ngai KL, Tsang KY. Phys Rev E 1999;60:4511.
[25] Ngai KL. J Phys C 2000;12:6437.
[26] Ngai KL, Rendell RW. Supercooled liquids, advances and novel applications. In: Fourkas JT, Kivelson D, Mohanty U, Nelson K, editors. ACS symposium series, vol. 676. Washington, DC: American Chemical Society, 1997. p. 45–66 (chap. 4).
[27] Ngai KL. J Chem Phys 1993;98:7588.
[28] Ngai KL, Plazek DJ. Rubber Chem Technol 1995;68:376.
[29] Ngai KL, Plazek DJ, Rendell W. Rheol Acta 1997;36:307.
[30] Kohlrausch R. Pogg Ann Phys 1847;12(3):393.
[31] Williams G, Watts DC. Trans Faraday Soc 1970;66:80.
[32] Ngai KL, Roland CM. Macromolecules 1994;27:2454.
[33] Böhmer R, Ngai KL, Angell CA, Plazek DJ. J Chem Phys 1993;99:4201.
[34] Johari GP, Ann NY. Ann N Y Acad Sci 1976;279:102.
[35] Ngai KL. J Chem Phys 1998;109:6982.
[36] Ngai KL. Phys Rev E 1998;57:7346.
[37] Ngai KL. Macromolecules 1999;32:7140.
[38] Yamamuro O, Tsukushi I, Lindqvist A, Takahara S, Ishikawa M, Matsuo T. J Phys Chem 1998;102:1605.
[39] Bu HS, Aycock W, Cheng SZD, Wunderlich B. Polymer 1988; 29:1485 [see also World Wide Web at URL http://web.utk.edu/~athas/databank/intro.html].
[40] McCrum NG, Read BE, Williams G. Anelastic and dielectric effects in polymeric solids. London: Wiley, 1967 [New York: Dover, 1991].
[41] Schönhals A. J Chem Phys, submitted.
[42] Plazek DJ. Polym J 1980;12:43.
[43] Rendell RW, Ngai KL, Mashimo S. J Chem Phys 1987;87:2359.
[44] Dixon PK. Phys Rev B 1990;42:8179.
[45] Stockmayer WH. IEEE Trans Electric Insul 1985;EI-20:923.
[46] Hall CK, Helfand E. J Chem Phys 1982;77:3275.
[47] Ngai KL, Rendell RW. J Non-Cryst Solids 1991;131–133:942.
[48] Kim EG, Mattice WL. J Chem Phys 1994;101:6242.
[49] Mashimo S, Nozaki R, Yagihara S, Takeishi J. J Chem Phys 1982;77:6259.
[50] Arbe A, Colmenero J, Gómez, Richter D, Farago B. Phys Rev Lett 1999;60:1103.
[51] Donth E, Schröter K, Kahle S. Phys Rev Lett 1999;60:1099.
[52] William G. Adv Polym Sci 1979;33:60.
[53] Liggat J. In: Brandrup J, Immergut EH, editors. Polymer handbook. New York: Wiley, 1975. p. II-459.
[54] Fischer EW, Donth E, Steffen W. Phys Rev Lett 1992;68:2344.
[55] Tracht U, Wilhelm M, Heuer A, Feng H, Schmidt-Rohr K, Spiess HW. Phys Rev Lett 1998;81:2727.
[56] Rizos AK, Ngai KL. Phys Rev E 1999;59:612.
[57] Knoff WF, Hopkins IL, Tobolsky AV. Macromolecules 1971;6:750.
[58] Santangelo PG, Ngai KL, Roland CM. Polymer 1998;39:681.